Polymer Journal
https://doi.org/10.1038/s41428-026-01152-x

ORIGINAL ARTICLE

Optimization of mechanochemical reactions through cellulose transacylation with vinyl laurate

Jacqueline Lease[1,2] · PeiQin Tan[3] · KaiXian Ng[1,3] · Mohammed A. A. Farid[4] · Yoshito Andou[1,2]

Received: 5 December 2025 / Revised: 10 January 2026 / Accepted: 12 January 2026

Abstract

Cellulose esters with long-chain alkyl groups are promising sustainable materials because their hydrophobicity and thermal stability can be tuned through chemical modification. We report a mechanochemical transacylation method for synthesizing cellulose laurates using vinyl laurate in a dimethyl sulfoxide/sodium hydroxide medium. The process enables the efficient modification of 0.81 g of cellulose and yields products with degrees of substitution ranging from 0.50 to 2.94 under different designated conditions. Structural analysis by Fourier transform infrared spectroscopy (FTIR) and X-ray diffraction (XRD) confirmed successful esterification and reduced crystallinity. The physical properties varied systematically with substitution level, with higher substitution improving thermal stability and reducing wettability, providing opportunities to tailor performance. Response surface methodology, which is based on a five-level, four-factor central composite rotatable design, was applied to study the interactive effects of synthesis parameters and optimize the degree of substitution. The experimental results closely matched the predicted values with 97.3% accuracy, demonstrating the robustness of the approach. This study establishes a green and reproducible route for producing functional cellulose esters with potential applications in bioplastics.

Intoroduction

In the past few years, growing environmental threats and the depletion of fossil fuels have heightened interest in the development of sustainable and biodegradable materials, especially bioplastics [1]. This is because plastic has emerged as a pivotal material in modern life owing to its remarkable versatility and broad range of uses. Unfortunately, plastic that is not managed properly after disposal becomes a significant environmental issue.

Cellulose, the most abundant natural polymer derived from lignocellulosic material, has attracted significant attention as a biodegradable alternative to fossil fuel plastics. Despite its potential, the use of cellulose is significantly limited because of its strong inter- and intramolecular hydrogen bonding. The formation of highly aligned supramolecular structures prevents cellulose from melting and dissolving in common solvents, making its processing challenging [2–4]. However, by introducing various substituent groups, cellulose derivatives with designated properties can be obtained. Cellulose modifications, particularly esterification, pave the way for a broad range of cellulose applications [5].

Mechanochemical esterification has recently emerged as a promising method for modifying cellulose because of its numerous advantages. This approach significantly reduces the need for harmful solvents, making the process more environmentally friendly and in line with green chemistry

Supplementary information The online version contains supplementary material available at https://doi.org/10.1038/s41428-026-01152-x.

✉ Yoshito Andou
ando.yoshito784@mail.kyutech.jp

[1] Department of Life Science and Systems Engineering, Graduate School of Life Science and Systems Engineering, Kyushu Institute of Technology, 2-4 Hibikino Wakamatsu-ku, Kitakyushu, Fukuoka 808-0196, Japan

[2] Collaborative Research Centre for Green Materials on Environmental Technology, Kyushu Institute of Technology, 2-4 Hibikino Wakamatsu-ku, Kitakyushu, Fukuoka 808-0196, Japan

[3] Department of Bioprocess Technology, Faculty of Biotechnology and Biomolecular Sciences, Universiti Putra Malaysia, Serdang, Selangor Darul Ehsan 43400, Malaysia

[4] Laboratory of Biopolymer and Derivatives, Institute of Tropical Forestry and Forest Products (INTROP), Universiti Putra Malaysia, Serdang, Selangor Darul Ehsan 43400, Malaysia

Published online: 04 March 2026

principles. Compared with traditional chemical processes, mechanochemical methods also offer energy savings while operating at low temperatures and with minimal solvent [6].

According to previous literature, Hou et al. [7, 8] demonstrated that the mechanochemical esterification of cellulose using pyridine showed promising melting processability. Additionally, mechanochemistry facilitates the synthesis of novel cellulose derivatives that are difficult to achieve through conventional methods. These benefits make mechanochemistry an attractive and sustainable alternative for cellulose modification. However, pyridine remains toxic and has an unpleasant odor.

A promising alternative to anhydride syntheses is the transacylation of cellulose using vinyl esters. Transacylation plays a key role in the sustainable utilization of ester derivatives, such as the production of polyesters [9–11] and biodiesel [12, 13] from natural resources. In biodiesel production, a conversion rate of approximately 80% can be achieved within a minute [14]. In addition, some previous studies have demonstrated that cellulose can dissolve in DMSO/DBU/CO_2 [15] and DMAc/LiCl/DBU [16] and react with various vinyl esters. However, most of these reactions require a large amount of solvent and a large excess of substrate to achieve a high degree of substitution.

In this work, the transacylation of cellulose with vinyl laurate was performed in a NaOH/DMSO solvent system via a mechanochemical method to obtain cellulose laurate (CL) with various degrees of substitution (DS) while minimizing solvent usage. Because predicting the reaction conditions required to achieve targeted DS values is challenging, response surface methodology (RSM), implemented using Design-Expert 7.0 software, was employed to model and optimize the process. Vinyl laurate was selected as the acyl donor on the basis of an optimization study using vinyl esters with different alkyl chain lengths, which demonstrated that long-chain acyl donors provide higher reaction efficiency than short-chain analogs under mechanochemical conditions (Table S2). In addition, vinyl laurate is a bioderived and readily available reagent, and its vinyl ester structure facilitates efficient acyl transfer, enabling systematic control of DS and broadening the potential utilization of cellulose through tunable material properties if the model created is valid.

Experimental section

Materials

Microcrystalline cellulose (MCC) powder from cotton linter with a particle size of 38 μm, dimethyl sulfoxide (DMSO), and sodium hydroxide (NaOH) pellets were obtained from Wako Pure Chemical Industry, Osaka, Japan. The vinyl laurate used as an acylating agent was obtained from Sigma–Aldrich (St. Louis, MO, USA). Different concentrations of aqueous NaOH solution (1, 2, 3, 4, and 5 M) were prepared using distilled water. All the reagents were received and utilized without further treatment.

Methods

Experimental design

The cellulose transacylation process was performed to determine the optimal conditions for achieving the highest DS, considering factors such as reaction time (X_1), reaction temperature (X_2), volume of DMSO (X_3), and concentration of NaOH (X_4). In this study, a central composite rotatable design (CCRD) with five levels and four factors was utilized in Design-Expert 7.0 software, necessitating the completion of 30 experiments. The total experiment count was calculated based on Eq. (1)[17]:Top of Form

$$N = 2^a + 2a + a_c = 2^4 + (2 \times 4) + 6 = 30 \quad (1)$$

where N represents the total number of experiments, a denotes the number of variables, and a_c is the number of replicates.

This design included 16 factorial points, 8 axial points, and 6 center points, and all the factors were arranged to 5 coded levels: -α, − 1, 0, +1, and + α[18]. Thus, the cellulose transacylation process involved the manipulation of variables and their respective levels. For instance, time (5 to 65 min), temperature (50 to 125 °C), concentration of NaOH (1 to 5 M), and volume of DMSO (0 to 20 mL) were used.

RSM encompasses statistical techniques employing a polynomial model based on a low-degree polynomial function, as illustrated in Eq. (2):

$$Y = f(X_1, X_2, X_3, X_4, \cdots, X_k) \quad (2)$$

Y is the relationship among the response variables, f is a function involving cross-products of the polynomial terms, and X_1, X_2, X_3, X_4, …, X_k represents the independent variables. The quadratic model [19], which serves as a polynomial function for predicting optimal points, is expressed accordingly (Eq. 3):

$$Y = b_0 + \sum_{i=1}^{n} biXi + \sum_{i=1}^{n} biiXi^2 + \sum_{i=1}^{n-1} \sum_{j=i+1}^{n} bijXiXj \quad (3)$$

where Y signifies the response, b_0 is the constant coefficient, bi indicates the linear coefficients, b_{ii} denotes the quadratic coefficients, b_{ij} is the coefficient of the second-

order interaction, n indicates the number of independent variables, and x_i and x_j represent the coded values corresponding to the independent variables.

Transacylation of cellulose with vinyl laurate

Scheme 1 outlines the mechanochemical transacylation process for modifying cellulose with vinyl laurate in the NaOH/DMSO system. MCC (0.81 g; 5 mmol), 6.79 g of vinyl laurate (30 mmol), 2 mL of NaOH at various concentrations (1, 2, 3, 4, and 5 M), and multiple volumes of DMSO (5, 10, 15, and 20 mL) were added and kneaded in a magnetic mortar with a constant rotational speed of 100 rpm (100 VAC, 15 W). Additionally, the reaction temperature was varied using a ribbon heater, ranging from 25 to 125 °C, and the reaction time was adjusted from 5 to 65 min. During this reaction, acetaldehyde was generated as a byproduct from the vinyl ester, and therefore, all operations were performed in a well-ventilated fume hood to ensure safe handling of this volatile and flammable aldehyde. After the transacylation process, the product was washed in distilled water and then precipitated in methanol. Cellulose laurate (CL) was filtered and washed with methanol twice to completely remove unwanted substances. Next, CL was vacuum dried at 60 °C overnight. The DS of CL was determined using the neutralization titration method.

Unlike conventional solution-based transacylation, which is typically conducted in a round-bottom flask and requires relatively large solvent volumes to ensure sufficient mixing and stirring, the mechanochemical approach enables efficient reactions under low-solvent conditions. In conventional systems, reactions with very small amounts of solvent are difficult to perform because of poor mass transfer and the inability to maintain effective stirring, whereas the kneading-based mechanochemical process allows intimate contact between reactants even at reduced solvent volumes.

Results analysis

The analysis involved three main steps—ANOVA, regression modeling, and response surface plotting—to determine the optimal conditions for CL transacylation. A total of 30 randomized runs were conducted. Statistical and graphical evaluations were used to examine the effects of the four factors and their linear, quadratic, and cubic interactions on the esterification process. First, ANOVA ($p < 0.05$) was used to identify significant variables, where lower p values and higher F ratios indicated stronger influence [3, 4].

The experimental data were then fitted to first- or second-order polynomial models, with first-order equations derived from full factorial designs and second-order equations from CCRD data [20, 21]. Model performance was validated using R^2 and predicted versus experimental plots, where higher R^2 values (closer to 1) reflected better model accuracy and correlation.

Optimization of the criteria and validation

Using numerical optimization in Design-Expert 7.0, the optimal reaction conditions were identified on the basis of the desirability function (D), which ranges from 0 (least desirable) to 1 (most desirable). If any response fell outside its desirability range, the overall D value became zero. Experiments were then carried out under the suggested conditions, and the results obtained were compared with the software's predicted values to validate the model [22].

Characterization

Fourier transform infrared (FT-IR) spectroscopy

First, 2 mg of CL powder was mixed with 100 mg of spectroscopic grade potassium bromide (KBr) at a mass ratio of 1 to 50. The mixture was subsequently compacted into a pellet until a translucent film formed. FT-IR spectroscopy (Nicolet iS5, Thermo Fisher, Waltham, MA, USA) was utilized to record the IR spectra of pure cellulose and CL. The process involved the collection of 16 scans, and the spectra ranged from 4000 to 400 cm^{-1} with a resolution of 4 cm^{-1}.

X-ray diffraction (XRD) analysis

Wide-angle XRD analysis of CL was performed using a Rigaku Miniflex 600 diffractometer (Rigaku Analytical Devices, Inc., Waltham, MA, USA). The XRD pattern utilized Cu-Kα radiation ($\lambda = 0.154$ nm), operating at a voltage of 30 kV and a current of 15 mA. The CL powder was scanned in the 2θ range between 3° and 70° with a

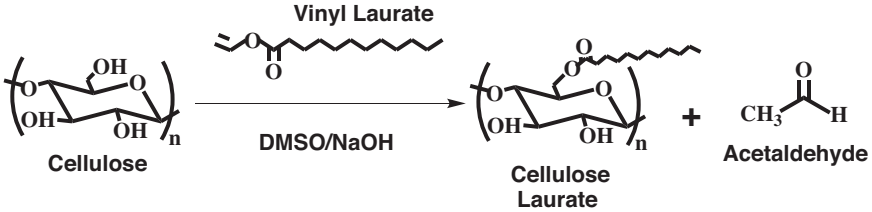

Scheme 1 Schematic depiction of the transacylation reaction of cellulose in DMSO/NaOH with vinyl laurate as an esterifying agent

scanning speed of 10° min^{-1}, and a step size of 0.02 was employed during the analysis.

Neutralization titration (JIS K0070:1992)

In the neutralization titration process, 0.3 g of CL was accurately measured and subjected to saponification using 5 mL of 0.1 M potassium hydroxide ethanol solution. The mixture was then heated at 65 °C for 4 h. After the solution was allowed to cool, it was titrated with a 0.1 M solution of hydrochloric acid, which resulted in the liberation of lauric acid. The DS values of CL were calculated by Eqs. 4 and 5 as follows[23, 24]:

$$n = [(V_0 - V_1) \times C_{HCl}]/1000 \quad (4)$$

$$DS = 162n/m - [(M - 1) \times n] \quad (5)$$

where the volumes of hydrochloric acid (mL) used for neutralizing the potassium hydroxide ethanol solution before and after the saponification of CL are denoted by V_0 and V_1, respectively. C_{HCl} is the molar concentration (in moles per liter) of the hydrochloric acid solution, m signifies the weight (g) of the CL, and M represents the molecular weight of the lauryl group. These DS values were obtained from experiments conducted in triplicate to ensure accuracy and reliability.

Thermal stability

The thermal properties of the cellulose esters were analyzed using an EXSTAR TG/DTA 7200 thermogravimetric analyzer (SII Nanotechnology Inc., Chiba, Japan). For this analysis, cellulose powder weighing between 5 and 10 mg was subjected to a controlled heating process under a nitrogen atmosphere. The flow rate of nitrogen was 100 mL per min. The temperature was gradually increased from 30 °C to 600 °C at a consistent rate of 10 °C per minute. This setup allowed for precise monitoring of the thermal degradation and stability of the cellulose samples under the specified conditions. The maximum decomposition temperature (T_{dmax}) was defined as the temperature corresponding to the maximum weight loss rate, determined from the peak of the derivative thermogravimetric (DTG) curve.

^{1}H NMR analysis

^{1}H NMR spectra were acquired on a 500 MHz JNM-ECZ500R spectrometer (JEOL Resonance, Tokyo, Japan). Approximately 10 mg of cellulose laurate was dissolved in 1 mL of $CDCl_3$ (deuterated chloroform) with stirring. From this solution, 500 µL was transferred into an NMR tube. Data collection was performed at 298 K using 16 scans, a 30° pulse, and a relaxation delay of 6 s. The DS of the CL was calculated on the basis of the following formula[25]:

$$DS = 10\,x\,I_{(CH3)}/\left(3x\,I_{(AGU)} + I_{(CH3}\right) \quad (6)$$

Cellulose film preparation using a hot press machine

The cellulose laurate powder was spread onto a PTFE sheet and then covered with another layer of PTFE. The PTFE sheets were subsequently inserted between aluminum plates. The sample was placed on the stage and pressed with a hot press machine (HC300-15 model, AS ONE Corporation, Osaka, Japan) at 130 °C under a pressure of 10 MPa for 15 min. After hot pressing, the stage and sample were cooled using a water cooling system, and they were removed once they had cooled to room temperature. This process resulted in the formation of cellulose laurate films.

Mechanical characterization

The mechanical properties of each film were assessed using a tensile and compression machine (Load Test Stand LTS-B, Minebea Mitsumi Inc., Tokyo, Japan) under tensile testing conditions. The Young's modulus, tensile strength, and elongation at break were determined. A 1 kN load cell and a crosshead speed of 10 mm/min were used, three replicate samples were tested for each film, and the standard deviations were reported.

Wettability of cellulose laurate films

Static water contact angle measurements of the cellulose ester films were conducted using a contact angle meter (DMs-401, Kyowa Electronic Instruments Co., Ltd., Tokyo, Japan). A 1 µL droplet of deionized water was deposited onto the surface of the cellulose laurate films, and the process was repeated five times for accuracy. Readings were taken for each sample to account for surface heterogeneity.

Results and discussion

Experimental design and synthesis of cellulose laurate

The effects of reaction time, temperature, NaOH concentration, and DMSO volume on the DS of CL were evaluated using RSM. Cellulose transacylation with vinyl laurate in the DMSO/NaOH system was carried out under various conditions on the basis of the design matrix, and the DS was determined by neutralization titration. FTIR and

Table 1 Experimental variable design matrix and experimental DS (DS_{Exp}) of CLs

Run	Time (min)		Temperature (°C)		Concentration of NaOH (M)		Volume of DMSO (mL)		DS_{Exp}
	Coded	Actual	Coded	Actual	Coded	Actual	Coded	Actual	
1	−1	20	1	100	1	4	1	15	2.94
2	−1	20	−1	50	−1	2	1	15	1.34
3	0	35	0	75	0	3	0	10	2.04
4	0	35	0	75	0	3	0	10	2.04
5	1	50	−1	50	1	4	1	15	1.86
6	1	50	−1	50	−1	2	−1	5	1.04
7	1	50	1	100	1	4	−1	5	2.50
8	1	50	1	100	−1	2	1	15	1.86
9	−1	20	−1	50	1	4	−1	5	1.04
10	−1	20	1	100	−1	2	−1	5	0.77
11	1	50	1	100	−1	2	−1	5	0.82
12	−1	20	−1	50	1	4	1	15	1.63
13	1	50	−1	50	1	4	−1	5	0.77
14	0	35	0	75	0	3	0	10	1.86
15	1	50	−1	50	−1	2	1	15	1.52
16	1	50	1	100	1	4	1	15	2.94
17	0	35	0	75	0	3	0	10	1.86
18	−1	20	1	100	−1	2	1	15	1.74
19	−1	20	−1	50	−1	2	−1	5	0.50
20	−1	20	1	100	1	4	−1	5	0.92
21	0	35	0	75	2	5	0	10	1.08
22	0	35	0	75	0	3	−2	0	0.25
23	−2	5	0	75	0	3	0	10	0.56
24	0	35	0	75	−2	1	0	10	0.77
25	0	35	0	75	0	3	0	10	1.86
26	0	35	−2	25	0	3	0	10	0.56
27	0	35	0	75	0	3	2	20	2.82
28	2	65	0	75	0	3	0	10	1.63
29	0	35	2	125	0	3	0	10	2.94
30	0	35	0	75	0	3	0	10	1.86

XRD analyses confirmed successful esterification, and ^{1}H NMR (Fig. S1–S4) further verified the DS values. The successful formation of cellulose laurate was confirmed by ^{1}H NMR spectroscopy.

The ^{1}H NMR spectra of cellulose laurate exhibit characteristic signals of lauryl side chains, including terminal methyl protons at approximately 0.88 ppm and methylene protons in the range of 1.5–2.5 ppm. The anhydroglucose unit (AGU) protons of the cellulose backbone are observed in the region of 3.0–5.5 ppm. Owing to the presence of long alkyl side chains, the AGU signals appear predominantly as a broadened envelope rather than as seven fully resolved resonances. With increasing degree of substitution, the AGU signals become slightly more discernible, as observed for Run 1 (DS = 2.94). However, complete resolution of individual AGU proton signals is still not achieved. This behavior is characteristic of long-chain cellulose esters and is attributed to reduced segmental mobility of the cellulose backbone and homogeneous local environments induced by dense alkyl substitution [26]. Accordingly, the DS was reliably determined from the integral ratios of alkyl-chain protons to AGU protons. These chemical shift assignments are consistent with those of previously reported cellulose fatty acid esters. The DS values determined by ^{1}H NMR showed only a slight deviation from those obtained by titration. However, the overall trends were consistent. After optimization, a predictive model was established to identify conditions that minimize DMSO usage, thereby improving process efficiency and enhancing environmental sustainability.

Table 1 presents the CCRD design matrix and the corresponding experimental results. ANOVA was used to

evaluate the model terms and determine the significance of the model equation. The DS values of samples prepared under identical conditions were similar, confirming the reproducibility of the method (Runs 14, 17, 25, and 20).

Characterization of cellulose laurates

The effectiveness of the modification reaction was initially revealed through chemical and structural analyses using FTIR and XRD.

FTIR analysis

The degree of esterification can be estimated by identifying the carbonyl group formation and hydroxyl group deformation of cellulose laurate using FTIR spectroscopy. Three samples from Runs 1, 3, and 9, whose DS values were 2.94, 2.04, and 1.04, respectively, were selected from Table 1 for chemical and structural analysis.

According to Fig. 1, a noticeable shift and reduction in the intensity of the characteristic peak of the hydroxyl group at 3475 cm^{-1} suggested that a substantial number of O–H groups were substituted by ester groups. This substitution was also associated with an increase in the intensity of the characteristic $–CH_2$ and $–CH_3$ asymmetric and symmetric stretching bands at 2923 and 2856 cm^{-1}, respectively, corresponding to the introduction of the long alkyl chain [27].

In addition, a new absorption peak at 1746 cm^{-1} could be observed compared to pristine MCC. This peak was attributed to the stretching vibration of the carbonyl groups (C = O)[28]. These observations confirmed the successful transacylation of cellulose with vinyl laurate according to the proposed protocol. Moreover, a higher DS corresponds to a higher intensity for C = O ester absorption, as indicated by the FTIR spectra [29]. In this context, the prominence of the C = O peak indicated the rate of the transacylation process.

Crystal structure of cellulose laurates

Figure 2 displays the crystal structures of MCC and CLs with various DSs. The XRD pattern of pristine MCC (DS = 0) was typical of cellulose I and exhibited four diffraction peaks at 2θ = 14.9, 16.9, 22.5, and 34.8° attributed to the $(1\bar{1}0)$, (110), (200), and (004) diffraction planes, respectively [30]. After the transacylation process, the characteristic peaks of the (101), $(10\bar{1})$, (002), and (040) planes weakened or disappeared, whereas a new broad XRD pattern at 2θ = 20° was clearly visible.

This new peak indicated the amorphous regions of the cellulose backbone [31]. The observed reduction and disappearance of the XRD pattern of cellulose I post-esterification could be attributed to the disruption of hydrogen bonds, which is in line with the FT-IR assignment. Furthermore, the low-angle peak at 2θ = 3° was attributed to the periodicity of the cellulose backbone chain because of the long alkyl side chains [32]. This scenario also proved the success of the transacylation reaction.

Thermal stability of cellulose laurates

The esterification of cellulose laurate resulted in a significant increase in thermal stability (Table 2 and Fig. S5). This study revealed that the thermal stability improved with

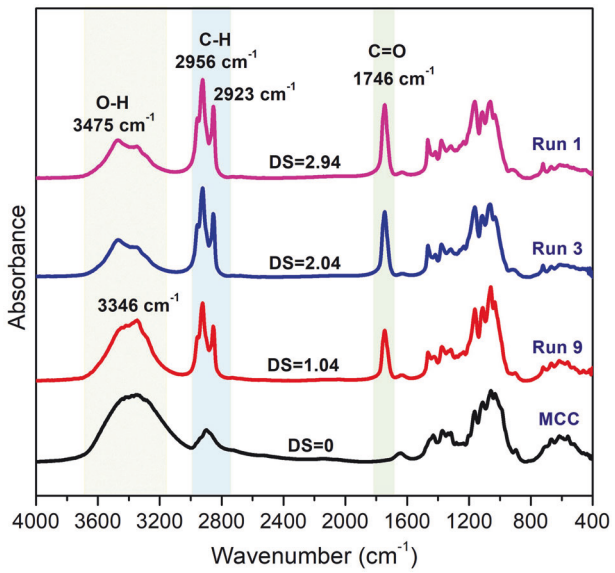

Fig. 1 FT-IR of MCC (DS = 0) and CLs (Runs 1, 3, and 9) with DSs of 1.04, 2.04, and 2.94, respectively

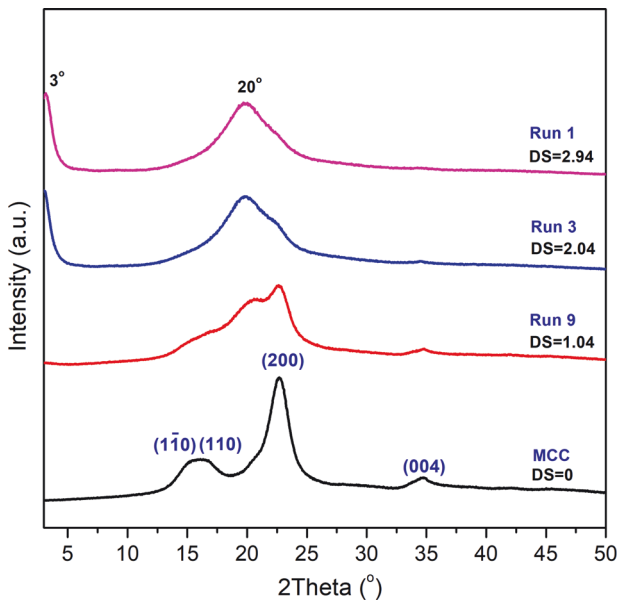

Fig. 2 XRD patterns of MCC (DS = 0) and CLs (Runs 1, 3, and 9) with various DSs

Table 2 Maximum decomposition temperature (T_{dmax}) of cellulose laurates with different DSs

Sample	T_{dmax} (°C)
MCC	335
DS = 1.04 (Run 9)	361
DS = 2.04 (Run 3)	367
DS = 2.94 (Run 1)	375

increasing DS. This increase in thermal stability could be attributed to the formation of a new crystalline structure by the long alkyl side chains of the laurate group, which has been reported to contribute to structural integrity and thermal resistance in similar cellulose derivatives [33]. The increase in thermal stability with DS was also explained by changes in the fundamental degradation mechanism of cellulose. Thermal decomposition of native cellulose was initiated by dehydration reactions between adjacent hydroxyl groups, followed by the formation of levoglucosan and rapid depolymerization [34].

As the DS increased, the number of free –OH groups decreased, which suppressed these dehydration pathways and greatly reduced the formation of levoglucosan. Consequently, the polymer was forced to degrade through less favorable ester-scission or random chain-scission routes, resulting in a higher onset temperature. Substitution with long laurate chains also disrupted the hydrogen-bonding network and increased hydrophobicity, shifting the thermal behavior from cellulose-like to polyester-like [35]. Similar DS-dependent improvements in thermal stability were observed for other long-chain cellulose esters prepared under mild transacylation conditions. This transformation revealed that different degrees of substitution resulted in varying levels of thermal stability.

Mechanical properties of cellulose laurates

The mechanical properties of CL films with different DS values (Fig. 3 and Table S3) clearly tend to increase with increasing DS. As the DS increases from 1.04 to 2.94, both the tensile strength and the Young's modulus gradually decrease, which is consistent with the expected reduction in hydrogen bonding and partial disruption of the crystalline regions caused by the introduction of bulky laurate groups. This structural alteration reduces the intermolecular packing efficiency and leads to lower stiffness and strength. In contrast, the elongation at break increases with DS, reflecting the greater molecular mobility and flexibility of the more highly substituted CL chains.

The elongation data show relatively wide variation, particularly at higher DSs, which may be related to subtle differences in film morphology or processing conditions,

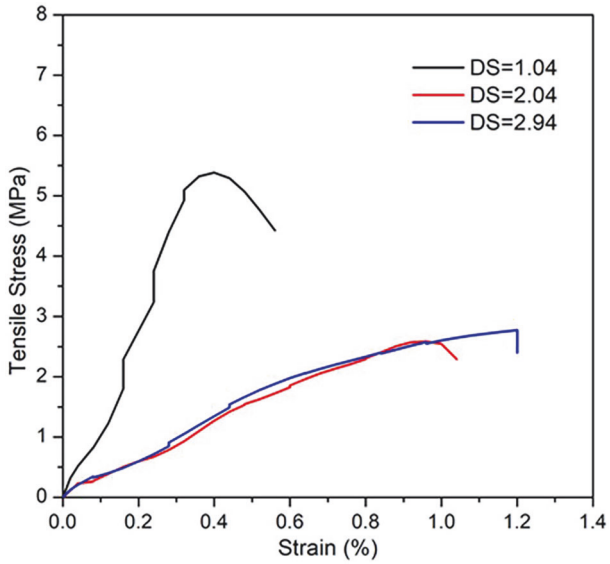

Fig. 3 Stress–strain curves of CL with DSs of 1.04, 2.04, and 2.94

Table 3 Water contact angles of CL films with DSs of 1.04 (Run 9), 2.04 (Run 3), and 2.94 (Run 1)

Sample	Water contact angles (°)
DS = 1.04 (Run 9)	106.8
DS = 2.04 (Run 3)	115.3
DS = 2.94 (Run 1)	120.0

such as thickness uniformity, dissolution behavior, or hot-pressing parameters such as the cooling rate. These factors can influence the deformation behavior of individual samples and may contribute to the observed scatter. Nevertheless, the overall mechanical trends remain consistent with those reported for long-chain cellulose esters, where higher substitution levels promote flexibility at the expense of rigidity. Continued refinement of film preparation conditions may help improve the reproducibility of ductility measurements in future work.

Wettability of cellulose laurate films

The water contact angles of the cellulose laurate films, as shown in Table 3 and Fig. S6, revealed that introducing lauryl groups onto the cellulose backbone induced hydrophobicity. As the degree of substitution increased, these lauryl groups increased the hydrophobicity of the material, increasing the water contact angle from 106.8° to 120°.

This improvement in surface hydrophobicity, along with enhanced thermal stability and mechanical properties, suggests the potential of cellulose for bioplastic applications. While higher hydrophobicity may contribute to better moisture resistance, further investigation beyond water contact angle measurements, such as water vapor

Table 4 Analysis of variance (ANOVA) for the response surface quadratic model

Source	Sum of squares	Mean square	*F* value	Prob > F
Model	15.59	1.11	9.48	0.0001[a]
Time (A)	0.22	0.22	1.83	0.1986[b]
Temperature (B)	0.37	0.37	3.18	0.0977[b]
Volume of DMSO (C)	2.16	2.16	18.44	0.0009[a]
Concentration of NaOH (D)	2.40	2.40	20.41	0.0006[a]
Residual	1.53	0.12	-	-
Lack of fit	1.53	0.15	-	-
Pure error	0.00	0.00	-	-
Cor Total	17.71	-	-	-

[a]Significant at "Prob>F" less than 0.05; [b]Nonsignificant at "Prob>F" greater than 0.05

transmission rate or long-term immersion tests, are necessary to fully assess its suitability for packaging applications. By controlling the degree of substitution, the material properties can be tuned to meet specific performance requirements.

Interpretation of modeling results

The esterification experiments produced DS values ranging from 0.25 to 2.94, depending on the reaction conditions, resulting in varying physical and mechanical properties. Data fitting using linear, quadratic, and cubic models, followed by ANOVA, revealed that a quadratic polynomial provided the best representation of the interactions, as summarized in Table 4.

The quadratic model equation for predicting the DS was as follows:

$$DS_{Exp} = -1.73920 + 0.057153\,A - 0.018975B + 0.11179\,C + 0.74354D + 1.78333\times10^{-4}AB - 1.14167\times10^{-3}AC + 2.70833\times10^{-3}AD + 7.35\times10^{-4}BC + 8.025\times10^{-3}BD + 0.010125CD - 7.79167\times10^{-4}A - 1.85\times10^{-5}B - 2.61250\times10^{-3}C - 0.21781D$$

ANOVA confirmed the model's significance, with a p value of 0.0001 and an F value of 9.48, indicating only a 0.01% probability that these results were due to noise [36]. The model showed strong predictive power, with an R^2 of 0.9108 and an adjusted R^2 of 0.8148 [37]. The standard deviation was low (0.34), and the signal-to-noise ratio was 12.33 (S/N > 4), demonstrating adequate precision and strong signal strength for exploring the design space.

According to Table 5, among the linear terms, NaOH concentration (D) had the strongest effect on the DS of CL, followed by DMSO volume (C) and reaction temperature (B). With respect to the quadratic terms, both temperature and NaOH concentration (BD) had significant effects

Table 5 Regression analysis of the CCRD model for the transacylation process with the associated statistical significance of each coefficient

Factor	Coefficient Estimate	Prob > F
Intercept	1.470	-
Time (A)	0.150	0.1986
Temperature (B)	0.200	0.0977
Volume of DMSO (C)	0.470	0.0009*
Concentration of NaOH (D)	0.670	0.0006*
A^2	−0.180	0.0189*
B^2	−0.012	0.8624
C^2	−0.065	0.3363
D^2	−0.220	0.0054*
AB	0.067	0.4489
AC	−0.086	0.3357
AD	0.041	0.6432
BC	0.092	0.3030
BD	0.200	0.0357*
CD	0.051	0.5646

*Significant at a P value less than 0.05

($p < 0.05$). Although variables with $p > 0.05$ were not statistically significant, they were retained in the model because of their potential relevance. Negative coefficient values indicated negative effects on the reaction, whereas all linear coefficients indicated positive effects on DS.

The interaction between the reaction temperature and NaOH concentration was particularly influential. The effects of reaction time, temperature, DMSO volume, and NaOH concentration on DS are illustrated in the 3D response surfaces and contour plots in Figs. 4 and 5, with the other parameters held at their median levels.

Figure 4a shows the interaction of reaction time and temperature, with the DMSO volume and NaOH concentration fixed at 15 mL and 3 M, respectively. A moderate DS of 1.87 was obtained even at 50 °C, whereas DS values above 2.5 were achieved at temperatures higher than 100 °C. The DS increased with increasing reaction time. After 50 min, the DS reached 1.87–2.08 at 50–75 °C and exceeded 2.5 at 100 °C even at 20 min. The increased reaction rate at high temperature is attributed to reduced water hydrolysis during transacylation[38].

Figures 4b and 4c illustrate the effects of DMSO volume and NaOH concentration with time, respectively. A higher DMSO volume (15 mL) was essential for obtaining DS values higher than 2.5, likely because of improved cellulose solubility from reduced mixture viscosity [39]. In contrast, low NaOH concentrations (< 1.25 M) resulted in low DS values (approximately 1.11), as shown in Fig. 4c.

The DS of CL increased proportionally with increasing NaOH concentration. NaOH acted as an intermediate to disrupt the original chain packing of cellulose by forming

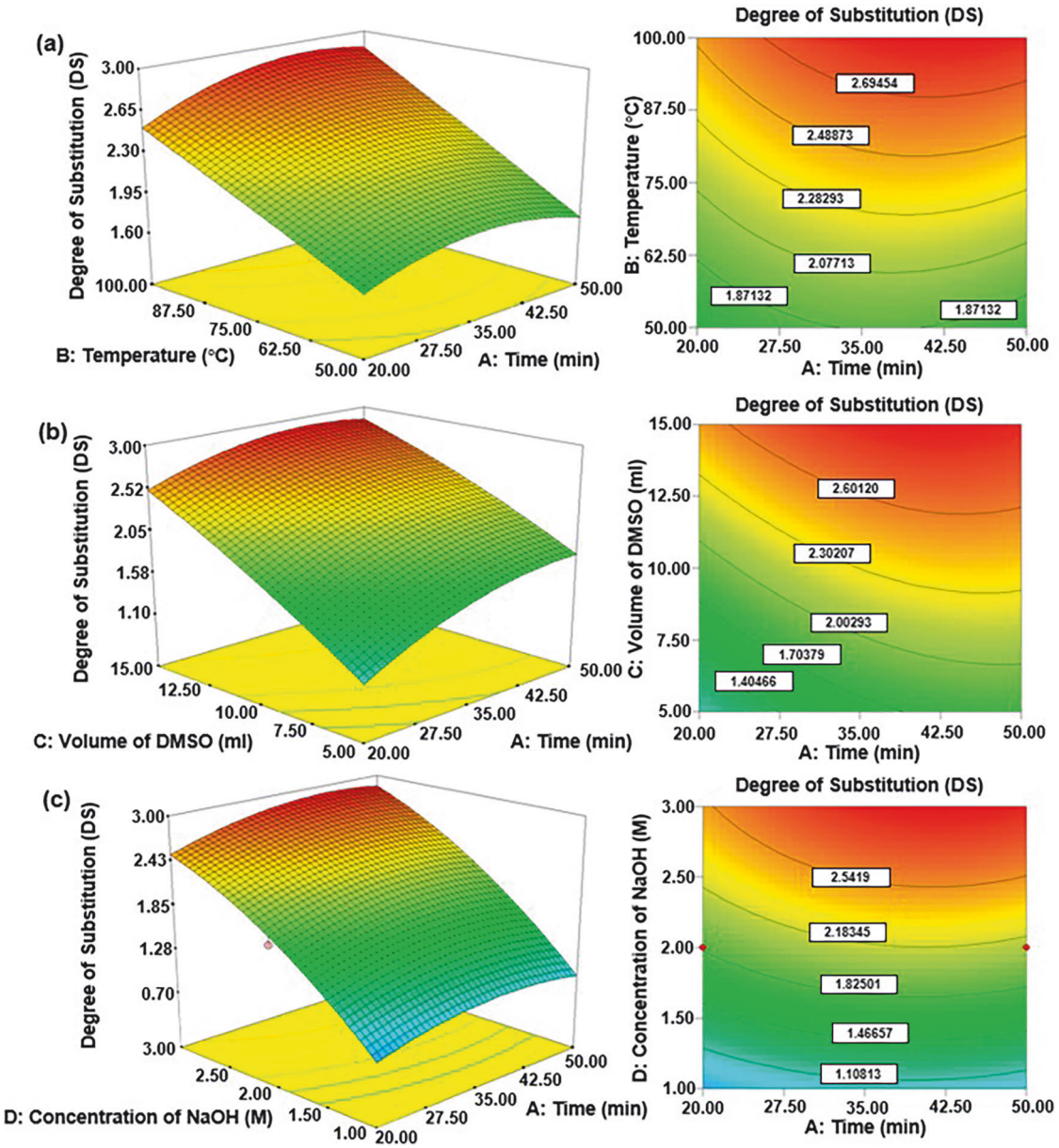

Fig. 4 3D and contour response surface plots showing the dependence of **a** reaction time and temperature, **b** reaction time and volume of DMSO, and **c** reaction time and concentration of NaOH on the DS of CLs

new hydrogen bonds between cellulose and NaOH hydrates. The cellulose–NaOH complex is then enveloped by DMSO, which reduces the aggregation of cellulose molecules. As a result, the solubility of the polymer improves, leading to more stable cellulose solutions [40]. Like the previous contour plot, the DS also increased as the reaction time increased for these two plots. Either a high volume of DMSO (> 10 mL) or a high temperature (> 75 °C) was required to produce CL with DS = 2.25.

The variations in the DS values of CL with respect to the volume of DMSO and temperature are shown in Fig. 5a. At low temperatures and low DMSO volumes, the DS values of the CLs were less than 2. As discussed in the previous section, the volume of DMSO and temperature were relatively significant. A lower DS was observed at low NaOH concentrations and low temperatures (Fig. 5b). The concentration of NaOH was the most significant factor according to the model. Therefore, low degrees of cellulose dissolution limit the rate of transacylation. Strong inter- and intramolecular hydrogen bonds of cellulose impeded the reaction from occurring.

Similar results are reported in Fig. 5c. The DS was very minimal at lower concentrations of NaOH (below 2 M) throughout the entire experimental DMSO volume range (from 5 to 15 mL). Various DS values (from 0.53 to 2.39) can

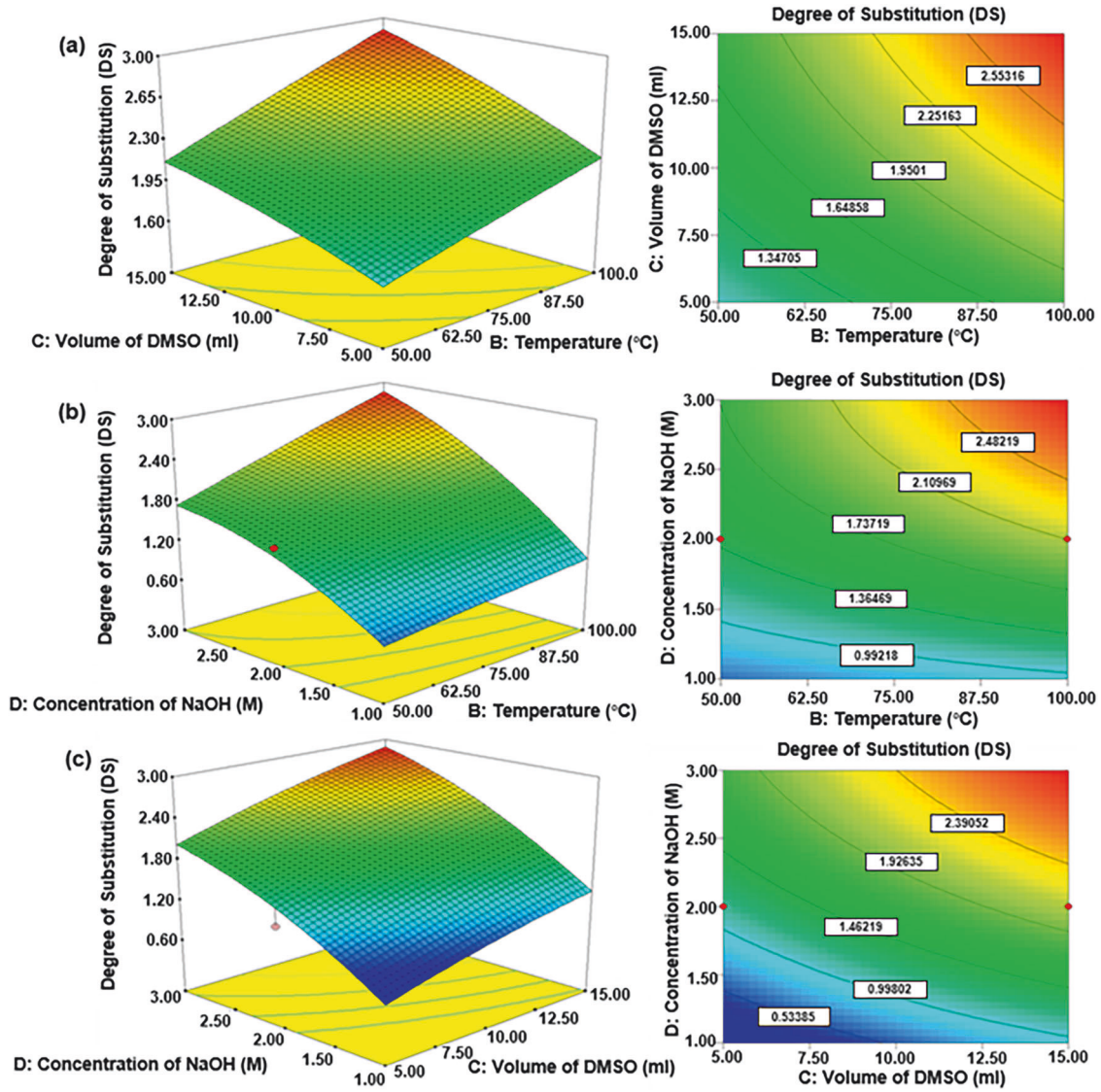

Fig. 5 3D and contour response surface plots showing the dependence of **a** volume of DMSO and temperature, **b** concentration of NaOH and temperature, and **c** volume of DMSO and concentration of NaOH on the DS of CLs

be attained by increasing the concentration of NaOH and volume of DMSO. The contour plots reported in Fig. 5a–c suggest that the influence of the reaction temperature, concentration of NaOH, and volume of DMSO on the substitution rate of the lauryl group onto the cellulose backbone was more significant than that of the reaction time.

Optimization and validation of the RSM

From the optimization process, the model generated an equation that allowed the prediction of reaction conditions for specific criteria. Because mechanochemical esterification requires minimal amounts of DMSO, a low DMSO content was set as the key parameter for achieving a high DS. Based on this constraint, the software estimated the optimal reaction time, temperature, NaOH concentration, and DMSO volume using the optimization results.

The second-order model describes how the response varies with the experimental level of each factor, enabling the identification of optimal conditions through response surface and contour plots. Table 6 summarizes the predicted optimal conditions for cellulose transacylation with vinyl laurate under low DMSO volume conditions.

The optimal conditions for maximizing CL synthesis were predicted as follows: a reaction time of 57 min, a temperature of 125 °C, a DMSO volume of 2 mL, and an NaOH concentration of 4.4 M. An experiment was then conducted to validate these predictions. The resulting DS was 2.15, differing from the model prediction by only 2.70%, confirming the high accuracy and reliability of the optimization model.

Table 6 Optimized reaction conditions for the transacylation process with a minimal amount of DMSO (approximately 2 mL), along with the percentage error between the predicted and experimental results

Sample	CL
Reaction Time (min)	57.00
Temperature (°C)	125.00
Volume of DMSO (mL)	2.60
Concentration of NaOH (M)	4.40
$DS_{Titration}$ (Predicted)	2.21
$DS_{Titration}$ (Experimental)	2.15
Error (%)	2.70

Conclusions

In this study, mechanochemical transacylation of cellulose with vinyl laurate was systematically investigated using a five-level, four-factor CCRD combined with response surface methodology (RSM). A broad range of DSs was successfully achieved, and the predicted optimal conditions showed excellent agreement with the experimental values, with a deviation of only 2.7%. The ability to precisely control DS through rational adjustment of reaction parameters provides a versatile strategy for tailoring the chemical structure of cellulose esters, which is directly linked to their mechanical and physical properties. Importantly, the present approach enables such structural tuning while minimizing solvent usage, highlighting its potential for solvent-efficient material synthesis.

Although alkali activation and acetaldehyde formation are intrinsic to the current vinyl ester-based system, these factors primarily define process boundaries rather than limiting the applicability of the material concept itself. The predictive framework established here offers clear guidance for future refinement of reaction conditions and reagent selection. Furthermore, the cellulose laurate produced in this work represents a promising biobased modifier or matrix component for bioplastic applications, including melt blending with biodegradable polymers and reactive blending strategies. Future work will explore alternative activation systems and acyl donors that prevent acetaldehyde formation while maintaining high mechanochemical efficiency. Coupling RSM with greener reagent selection and structure–property evaluation will further support the sustainable, application-driven development of cellulose esters for bioplastic applications.

Acknowledgements We thank JST Spring (Grant Number JPMJSP2154) for supporting this research work.

Author contributions The manuscript was written through the contributions of all the authors. All the authors have approved the final version of the manuscript.

Compliance with ethical standards

Conflict of interest The authors declare that they have no competing interests.

Publisher's note Springer Nature remains neutral with regard to jurisdictional claims in published maps and institutional affiliations.

References

1. Pei F, Liu L, Zhu H, Guo H. Recent Advances in Lignocellulose-Based Monomers and Their Polymerization. Polym. 2023;15:829 https://doi.org/10.3390/polym15040829.
2. Ishida T. Theoretical Investigation of Dissolution and Decomposition Mechanisms of a Cellulose Fiber in Ionic Liquids. J Phys Chem B. 2020;124:3090–3102. https://doi.org/10.1021/acs.jpcb.9b11527.
3. Zhang H, Lang J, Lan P, Yang H, Lu J, Wang Z. Study on the Dissolution Mechanism of Cellulose by ChCl-Based Deep Eutectic Solvents. Materials. 2020;13:278 https://doi.org/10.3390/ma13020278.
4. Satani H, Kuwata M, Shimizu A. Simple and environmentally friendly preparation of cellulose hydrogels using an ionic liquid. Carbohydr Res. 2020;494:108054. https://doi.org/10.1016/j.carres.2020.108054.
5. Wang Y, Wang X, Xie Y, Zhang K. Functional nanomaterials through esterification of cellulose: a review of chemistry and application. Cellulose. 2018;25:3703–3731. https://doi.org/10.1007/s10570-018-1830-3.
6. Kuga S, Wu M. Mechanochemistry of cellulose. Cellulose. 2019;26:215–225. https://doi.org/10.1007/s10570-018-2197-1.
7. Hou D-F, Li P-Y, Zhang K, Li M-L, Feng Z-W, Yan C, et al. Insight into the Feasibility of Fatty Acyl Chlorides with 10–18 Carbons for the Ball-Milling Synthesis of Thermoplastic Cellulose Esters. Biomacromolecules. 2024;25:1923–1932. https://doi.org/10.1021/acs.biomac.3c01354.
8. Hou D-F, Li M-L, Li P-Y, Zhou L, Zhang K, Liu Z-Y, et al. Efficient Conversion of Cellulose to Thermoplastics by Mechanochemical Esterification. ACS Sustain Chem Eng. 2023;11:7655–7663. https://doi.org/10.1021/acssuschemeng.2c07364.
9. Kenwright AM, Peace SK, Richards RW, Bunn A, MacDonald WA. Transesterification in poly(ethylene terephthalate) and poly(ethylene naphthalene 2, 6-dicarboxylate) blends; The influence of hydroxyl end groups. Polym. 1999;40:5851–5856. https://doi.org/10.1016/S0032-3861(98)00806-4.
10. Okabayashi R, Ohta Y, Yokozawa T. Synthesis of telechelic polyesters by means of transesterification of an A2 + B2 polycondensation-derived cyclic polyester with a functionalized

diester. Polym Chem. 2019;10:4973–4979. https://doi.org/10.1039/c9py00960d.
11. Cao X, Sun S, Peng X, Zhong L, Sun R, Jiang D. Rapid synthesis of cellulose esters by transesterification of cellulose with vinyl esters under the catalysis of NaOH or KOH in DMSO. J Agric Food Chem. 2013;61:2489–2495. https://doi.org/10.1021/jf3055104.
12. Mohd Johari SA, Ahmad Farid MA, Ayoub M, Rashidi NA, Andou Y (2024) Optimization and kinetic studies for biodiesel production from dairy waste scum oil via microwave assisted transesterification. Environ Technol Innov 34: https://doi.org/10.1016/j.eti.2024.103580
13. Farouk SM, Tayeb AM, Abdel-Hamid SMS, Osman RM. Recent advances in transesterification for sustainable biodiesel production, challenges, and prospects: a comprehensive review. Environ Sci Pollut Res. 2024;31:12722–12747. https://doi.org/10.1007/s11356-024-32027-4.
14. Monika, Banga S, Pathak VV (2023) Biodiesel production from waste cooking oil: A comprehensive review on the application of heterogenous catalysts. Energy Nexus 10: https://doi.org/10.1016/j.nexus.2023.100209.
15. Chen H, Yang F, Du J, Xie H, Zhang L, Guo Y, et al. Efficient transesterification reaction of cellulose with vinyl esters in DBU/DMSO/CO_2 solvent system at low temperature. Cellulose. 2018;25:6935–6945. https://doi.org/10.1007/s10570-018-2078-7.
16. Ding J, Li C, Liu J, Lu Y, Qin G, Gan L, et al. Time and energy-efficient homogeneous transesterification of cellulose under mild reaction conditions. Carbohydr Polym. 2017;157:1785–1793. https://doi.org/10.1016/j.carbpol.2016.11.063.
17. Aklilu EG, Adem A, Kasirajan R, Ahmed Y. Artificial neural network and response surface methodology for modeling and optimization of activation of lactoperoxidase system. S Afr J Chem Eng. 2021;37:12–22. https://doi.org/10.1016/j.sajce.2021.03.006.
18. Faraji N, Zhang Y, Ray A. Optimization of Lactoperoxidase and Lactoferrin Separation on an Ion-Exchange Chromatography Step. Separations. 2017;4:10 https://doi.org/10.3390/separations4020010.
19. Bacha EG. Response Surface Methodology Modeling, Experimental Validation, and Optimization of Acid Hydrolysis Process Parameters for Nanocellulose Extraction. S Afr J Chem Eng. 2022;40:176–185. https://doi.org/10.1016/j.sajce.2022.03.003.
20. Samaram S, Mirhosseini H, Tan CP, Ghazali HM, Bordbar S, Serjouie A. Optimisation of ultrasound-assisted extraction of oil from papaya seed by response surface methodology: Oil recovery, radical scavenging antioxidant activity, and oxidation stability. Food Chem. 2015;172:7–17. https://doi.org/10.1016/j.foodchem.2014.08.068.
21. Agu C, Menkiti M, Kadurumba C, Menkiti N. Process parameter optimization for transformer oil extraction from Terminalia catappa s eed using response surface methodology. J Chin Adv Mater Soc. 2015;3:328–344. https://doi.org/10.1080/22243682.2015.1088794.
22. Gunawan ER, Suhendra D. Four-Factor Response Surface Optimization of the Enzymatic Synthesis of Wax Ester from Palm Kernel Oil. Indonesian J Chem. 2010;8:83–90. https://doi.org/10.22146/ijc.21653.
23. Lease J, Kawano T, Andou Y. Effect of cellulose materials on the mechanochemical-assisted reaction system with oleic acid. RSC Adv. 2023;13:27558–27567. https://doi.org/10.1039/d3ra04715f.
24. Hou D-F, Li M-L, Yan C, Zhou L, Liu Z-Y, Yang W, et al. Mechanochemical preparation of thermoplastic cellulose oleate by ball milling. Green Chem. 2021;23:2069–2078. https://doi.org/10.1039/D0GC03853A.
25. Wen X, Wang H, Wei Y, Wang X, Liu C. Preparation and characterization of cellulose laurate ester by catalyzed transesterification. Carbohydr Polym. 2017;168:247–254. https://doi.org/10.1016/j.carbpol.2017.03.074.
26. Heinze T, Liebert T. Unconventional methods in cellulose functionalization. Prog Polym Sci. 2001;26:1689–1762. https://doi.org/10.1016/S0079-6700(01)00022-3.
27. Sejati PS, Obounou Akong F, Fradet F, Gérardin P. Wood Esterification by Fatty Acids Using Trifluoroacetic Anhydride as an Impelling Agent and Its Application for the Synthesis of a New Bioplastic. Materials. 2023;16:6830 https://doi.org/10.3390/ma16216830.
28. Gil Giraldo GA, Mantovan J, Marim BM, Kishima JO, Mali S. Surface Modification of Cellulose from Oat Hull with Citric Acid Using Ultrasonication and Reactive Extrusion Assisted Processes. Polysaccharides. 2021;2:218–233. https://doi.org/10.3390/polysaccharides2020015.
29. Zhao G, Wang F, Lang X, He B, Li J, Li X. Facile one-pot fabrication of cellulose nanocrystals and enzymatic synthesis of its esterified derivative in mixed ionic liquids. RSC Adv. 2017;7:27017–27023. https://doi.org/10.1039/c7ra02570j.
30. Guo Y, Wang X, Li D, Wang X, Sun R. Synthesis and characterization of hydrophobic long-chain fatty acylated cellulose and its self-assembled nanoparticles. Polym Bull. 2012;69:389–403. https://doi.org/10.1007/s00289-012-0729-7.
31. Kawano T, Andou Y. Synthesis and mechanical performance of thermoformable cellulose fatty acid esters using natural soap. RSC Adv. 2023;13:24286–24290. https://doi.org/10.1039/D3RA03833E.
32. Tanaka S, Iwata T, Iji M. Long/Short Chain Mixed Cellulose Esters: Effects of Long Acyl Chain Structures on Mechanical and Thermal Properties. ACS Sustain Chem Eng. 2017;5:1485–1493. https://doi.org/10.1021/acssuschemeng.6b02066.
33. Huang FY. Thermal properties and thermal degradation of cellulose tri-stearate (CTs). Polymers. 2012;4:1012–1024. https://doi.org/10.3390/polym4021012.
34. Lu Q, Yang XC, Dong CQ, Zhang ZF, Zhang XM, Zhu XF. Influence of pyrolysis temperature and time on the cellulose fast pyrolysis products: Analytical Py-GC/MS study. J Anal Appl Pyrolysis. 2011;92:430–438. https://doi.org/10.1016/j.jaap.2011.08.006.
35. Wen X, Wang H, Wei Y, Wang X, Liu C. Preparation and characterization of cellulose laurate ester by catalyzed transesterification. Carbohydr Polym. 2017;168:247 https://doi.org/10.1016/j.carbpol.2017.03.074.
36. Singh O, Panesar PS, Chopra HK. Response surface optimization for cellulose production from agro industrial waste by using new bacterial isolate Gluconacetobacter xylinus C18. Food Sci Biotechnol. 2017;26:1019–1028. https://doi.org/10.1007/s10068-017-0143-x.
37. Anggoro DD, Buchori L, Djaeni M, Hadiyanto DS, Shidqi A, et al. Optimization on The Hydrolysis Process of Cellulose from Corn Husk to Glucose with Activated Carbon Catalyst Sulfonated. J Phys Conf Ser. 2021;1858:012088 https://doi.org/10.1088/1742-6596/1858/1/012088.
38. Lease J, Kawano T, Andou Y. Esterification of Cellulose with Long Fatty Acid Chain through Mechanochemical Method. Polymers. 2021;13:4397 https://doi.org/10.3390/polym13244397.
39. Ren F, Wang J, Yu J, Zhong C, Xie F, Wang S. Dissolution of Cellulose in Ionic Liquid–DMSO Mixtures: Roles of DMSO/IL Ratio and the Cation Alkyl Chain Length. ACS Omega. 2021;6:27225–27232. https://doi.org/10.1021/acsomega.1c03954.
40. Qi H, Yang Q, Zhang L, Liebert T, Heinze T. The dissolution of cellulose in NaOH-based aqueous system by two-step process. Cellulose. 2011;18:237–245. https://doi.org/10.1007/s10570-010-9477-8.